Research in Astronomy and Astrophysics, 24:095022 (12pp), 2024 September https://doi.org/10.1088/1674-4527/ad74dc

Sunspot Group Detection and Classification by Dual Stream Convolutional Neural Network Method

Nyasha Mariam Mkwanda[1,2], Weixin Tian[2,3], and Junlin Li[1]
[1] Hubei Key Laboratory of Intelligent Vision Based Monitoring for Hydroelectric Engineering, China Three Gorges University, Yichang 443002, China; nyashamariam@icloud.com
[2] College of Computer and Information Technology, China Three Gorges University, Yichang 443002, China; t_wxin@126.com
Received 2024 March 28; revised 2024 August 8; accepted 2024 August 20; published 2024 September 20

Abstract

The automatic detection and analysis of sunspots play a crucial role in understanding solar dynamics and predicting space weather events. This paper proposes a novel method for sunspot group detection and classification called the dual stream Convolutional Neural Network with Attention Mechanism (DSCNN-AM). The network consists of two parallel streams each processing different input data allowing for joint processing of spatial and temporal information while classifying sunspots. It takes in the white light images as well as the corresponding magnetic images that reveal both the optical and magnetic features of sunspots. The extracted features are then fused and processed by fully connected layers to perform detection and classification. The attention mechanism is further integrated to address the "edge dimming" problem which improves the model's ability to handle sunspots near the edge of the solar disk. The network is trained and tested on the SOLAR-STORM1 data set. The results demonstrate that the DSCNN-AM achieves superior performance compared to existing methods, with a total accuracy exceeding 90%.

Key words: Sun: magnetic fields – Sun: flares – (Sun:) sunspots – DSCNN – Attention mechanism – Edge dimming

1. Introduction

Sunspots represent temporary blots on the photosphere of the Sun which are darker than the surrounding regions. These are linked to solar activity levels and could reflect space climate status. The detection and classification of sunspots is of great importance in space weather prediction (Ndacyayisenga et al. 2021; Lee et al. 2012; Guo et al. 2014; Yi et al. 2021; Prasad et al. 2022) and in satellite operation and telecommunications (Kucuk et al. 2017; Abed et al. 2021). Despite the use of deep learning (Goodfellow et al. 2016) and other machine learning methods for sunspot group detection and classification, accurately identifying and classifying sunspots remain challenging particularly with large data sets or images with complex backgrounds (Schuh & Angryk 2014; Junior & Luisir 2019). Addressing these challenges is crucial as highlighted by Jaeggli & Norton (2016) who identified significant gaps in our understanding of solar active region (AR) statistics.

The edge dimming effect of sunspots is an important factor affecting the accuracy of sunspot identification and classification. It is caused by factors such as projection when a sunspot group approaches the edge of the solar surface. As a result, the characteristics of the white light map of the sunspot group become blurred and the accuracy of magnetic field measurement decreases.

The Mount Wilson classification scheme is a classification scheme on the magnetic pole distribution of sunspot groups which is of high value as it shows the relationship between the complex magnetic pole structure of sunspot groups and the formation of solar storms. The Mount Wilson classification scheme requires a comprehensive analysis of different dimensions of feature information to determine the magnetic type of a sunspot group. The process begins with observing the structure of the sunspot group using a white light map followed by examining the magnetic pole distribution on the corresponding magnetic map. These observations are then combined to determine the magnetic type of the sunspot group.

To address the challenges of the "edge dimming" problem in sunspot detection and classification, we propose a dual stream convolutional neural network (DSCNN) method inspired by the Mount Wilson scheme. One branch of the network is dedicated to extracting features from white light images while the other branch extracts features from magnetic maps. These distinct types of features are fused in the fully connected layer. The dual stream architecture allows the model to capture both fine-grained details and broader contextual information, leading to better generalization across diverse sunspot appearances. Our model is optimized for real-time processing, ensuring that

[3] corresponding author.

it can be deployed in operational settings where timely detection is critical.

The attention mechanism (Xu et al. 2016; Anderson et al. 2018) is a fine tuning technique for tuning weights. It allows the model to focus on the most relevant parts of the input data, ensuring that critical information such as sunspot edge details is adequately considered. The attention mechanism is adopted in this paper to mitigate the "edge dimming" issue by ensuring that edges receive appropriate attention, leading to an improved overall performance.

The rest of the paper is organized as the following: Section 2 discusses methods from related work highlighting previous studies and their methodologies and how our work builds upon and differs from them. Section 3 focuses on the SOLAR-STORM1 data set detailing its composition. Section 4 presents the architecture of the DSCNN including the attention mechanism and its implementation. Section 5 delves into the experiment and discussion describing the experimental setup, results, comparisons with existing methods and the impact of the attention mechanism on performance. Finally, Section 6 concludes the paper by summarizing the key findings, contributions and potential future work directions.

2. Related Work

In recent years an increasing number of space missions have led to a rapid accumulation of solar activity data. With the development of automatic sunspot recognition technology, an increasing number of studies are devoted to the automatic classification of sunspots. The proposed methods can be roughly categorized into traditional methods and deep learning methods.

Traditional methods include machine learning methods and other statistics-based method. Nguyen et al. (2005) proposed a system combining rough set theory and hybrid methods to preprocess and classify sunspot images, leveraging domain knowledge to improve standalone methods. Though feasible, the method suffers from complexity when faced by an increased workload. Moreover, (Majed et al. 2010) introduces an automated method for classifying sunspot groups using Support Vector Machines (SVMs). The technique involves several phases: extracting the solar disk from full-disk images, binarizing and smoothing the image, segmenting sunspots and grouping them, extracting attributes from each group and finally classifying the sunspot groups using a one-against-all SVM approach. Similarly, Nguyen et al. (2006) used decision trees and clustering methods which despite their historical significance require manual feature extraction making them slower and more labor-intensive. This shortcoming was also faced by Colak & Qahwaji (2008) who developed a hybrid system integrating the McIntosh classification method with image processing and neural networks to detect and classify sunspots. Their approach enhanced both accuracy and efficiency of sunspot detection by leveraging statistical techniques including fractional-order calculus, thresholding and attribute extraction. Even though it led to more accurate identification of sunspots, the method is complex and requires more computational time. Similarly, Veeramani & Sudhakar (2024) blended global and local thresholding to improve accuracy and robustness in the detection and classification of sunspots. While the traditional approaches can offer some advantages in terms of detection precision, they also face challenges related to parameter tuning and implementation and do not have the ability to process complicated solar images.

Recent advancements in deep learning have significantly improved the performance of detection and classification of sunspots. Stenning et al. (2012) utilized mathematical morphology for feature extraction in automated classification systems combining traditional image processing techniques with modern machine learning algorithms to handle the complex shapes of sunspots. Fang et al. (2019) developed a deep learning algorithm that achieved high classification accuracy using white light images. More so, Ling et al. (2020) further improved upon these methods by combining reprocessing, thresholding and morphological operations for detection and comprehensive feature extraction for detailed analysis and detection of sunspots. Nevertheless, this approach remains sensitive to threshold settings it is computationally complex. Tang et al. (2021) took these advancements further by developing an ensemble model using multiple deep-learning algorithms, leveraging diverse perspectives from different models to uncover new insights. However, this approach still required substantial computational resources. Herrera et al. (2021) created a unique model that gave insights into the various patterns of the sunspots' magnetic dynamo that drives solar activity maxima and minima. They applied machine learning algorithms to the World Data Centers newly constructed annual sunspot time series. Additionally, Chola & Benifa (2022) focused on utilizing deep convolutional neural networks (CNNs) for the detection and classification of sunspots in solar images. Despite offering significant advantages in terms of accuracy and automation this method presented challenges related to threshold sensitivity, noise sensitivity, computational complexity as well as feature selection. Mourato et al. (2024) introduced a hybrid method that leveraged deep learning techniques to identify and delineate sunspots. Though this method provides a detailed and pixel-level classification of sunspots, the model requires substantial computational resources including high-performance GPUs for both training and inference.

The deep learning methods provide a promising approach for sunspot detection and classification. With massive solar data sets being crafted, deep learning methods have achieved far better performance than traditional methods. The main issue for the deep learning methods is to further improve classification accuracy currently. As mentioned earlier, the "edge dimming" phenomenon significantly impacts classification accuracy and this paper aims to address it using a deep learning approach.

3. Dataset

The data set we used is the SOLAR-STORM1 sunspot group data set provided by the space environment artificial intelligence early warning innovation workshop, Observational Image Magnetic Classification Dataset (Fang et al. 2019). This data set is based on the magnetic type classification scheme of the Mount Wilson sunspot group and is divided into two parts: white light images and magnetic images. Each white light image part or magnetic image part contains three types: Alpha, Beta and Betax. It can be downloaded publicly from the Tianchi Experiment. The data set consists of images from the Helioseismic and Magnetic Imager (HMI) labeled as space-weather HMI active region patches (SHARP) captured at 720 s intervals. Each file follows the naming convention: `hmi.sharp_720s.num.YYYYMMDD_hhmmss_TAI.magnetogram.Fits`, where "Fits" stands for Flexible Image Transport System which is a digital file format used to store, transmit and manipulate scientific images. To ensure no object intersection occurs between the test set and the training set after data set division, the experimental data in this study are divided into the test set and the training set according to the observation objects. The data set consists of a total of 14,469 data samples, each containing two images: magnetic and white light maps. These include:

1. 4709 magnetic field maps and white light maps of Alpha sunspots: accounting for 32.54% of the data set.
2. 7353 magnetic field maps and white light maps of Beta sunspots: accounting for 50.82% of the data set.
3. 2407 magnetic field maps and white light maps of Betax sunspots: accounting for 16.64% of the data set.

Due to the slow evolution of the sunspot groups, the sunspot groups maintain the same magnetic type within a certain period of time. Consequently, most of the sunspot groups exhibit high magnetic similarity when observed, posing challenges for the model's classification accuracy. Figure 1 below shows some of the sunspots that one can find in our data set.

4. Method

To address the edge dimming problem often encountered in sunspot images, a DSCNN-AM architecture is proposed for the group classification of sunspots. This method integrates the ResNet50 model as the backbone and then incorporates attention mechanisms. The model is built using a pre-trained model in Keras, which includes 10 pre-trained models for image classification trained on ImageNet data. The construction process involves creating the ResNet50 branches (loading ImageNet weights) for extracting features from white light and magnetic images named the white light feature branch and the magnetic image feature branch respectively. After feature extraction, the two feature sets are concatenated, flattened and input into a fully connected layer with L2 regularization. The output then passes through another fully connected layer with Dropout before being classified using Softmax.

4.1. Network Architecture

The network structure is displayed in Figure 2 illustrates the DSCNN structure. We input the white light image and the magnetic image separately into the network, each entering different branches without sharing CNN weights. This results in two distinct feature vectors which are then concatenated and passed through a fully connected layer. The red arrows indicate the shortcut connections that bypass certain layers connecting earlier layers directly to later layers within the convolutional stages. These connections represent the residual units typical in a ResNet architecture which help improve gradient flow during training. Softmax is subsequently used for classification.

4.2. DSCNN-AM

In order to further enhance the classification accuracy of the DSCNN and mitigate the negative impact of edge dimming, we incorporate an attention mechanism into the model. This allows the network to assign greater weight to the sunspot group areas when processing images, effectively filtering out the effects of the edge dimming phenomena. In our modified model drawn in Figure 3, ResNet50 is integrated with the attention mechanism.

Specifically, ResNet50 is integrated with both Squeeze-and-Excitation Network (SE-Net) and Convolutional Block Attention Module (CBAM) attention mechanisms. The SE-Net introduces channel-wise attention, while CBAM combines both channel-wise and spatial attention, ensuring that the model can focus on the most relevant parts of the input images. This integration enhances the model's ability to emphasize important features leading to improved classification accuracy.

4.2.1. ResNet Unit Combined with Squeeze-and-Excitation Network (SE-Net)

The Squeeze-and-Excitation Network, first introduced by Hu et al. (2018), introduces channel-wise attention that recalibrates feature responses by explicitly modeling the interdependencies between the channels of convolutional features. The ResNet network is composed of multiple residual units. The process of images entering each residual module is the process of feature extraction. In order to use the attention mechanism in each feature extraction process, the attention mechanism must be integrated into the residual module. The structure of the residual module combined with SE-Net is illustrated in Figure 4. When the feature map X enters the residual module, it is processed by SE-Net to form a refined feature map $\tilde{X}$. This refined feature map is then added to the initial feature map to produce the final feature map. This integration ensures that the network focuses more on relevant areas thereby improving the accuracy of sunspot classification.

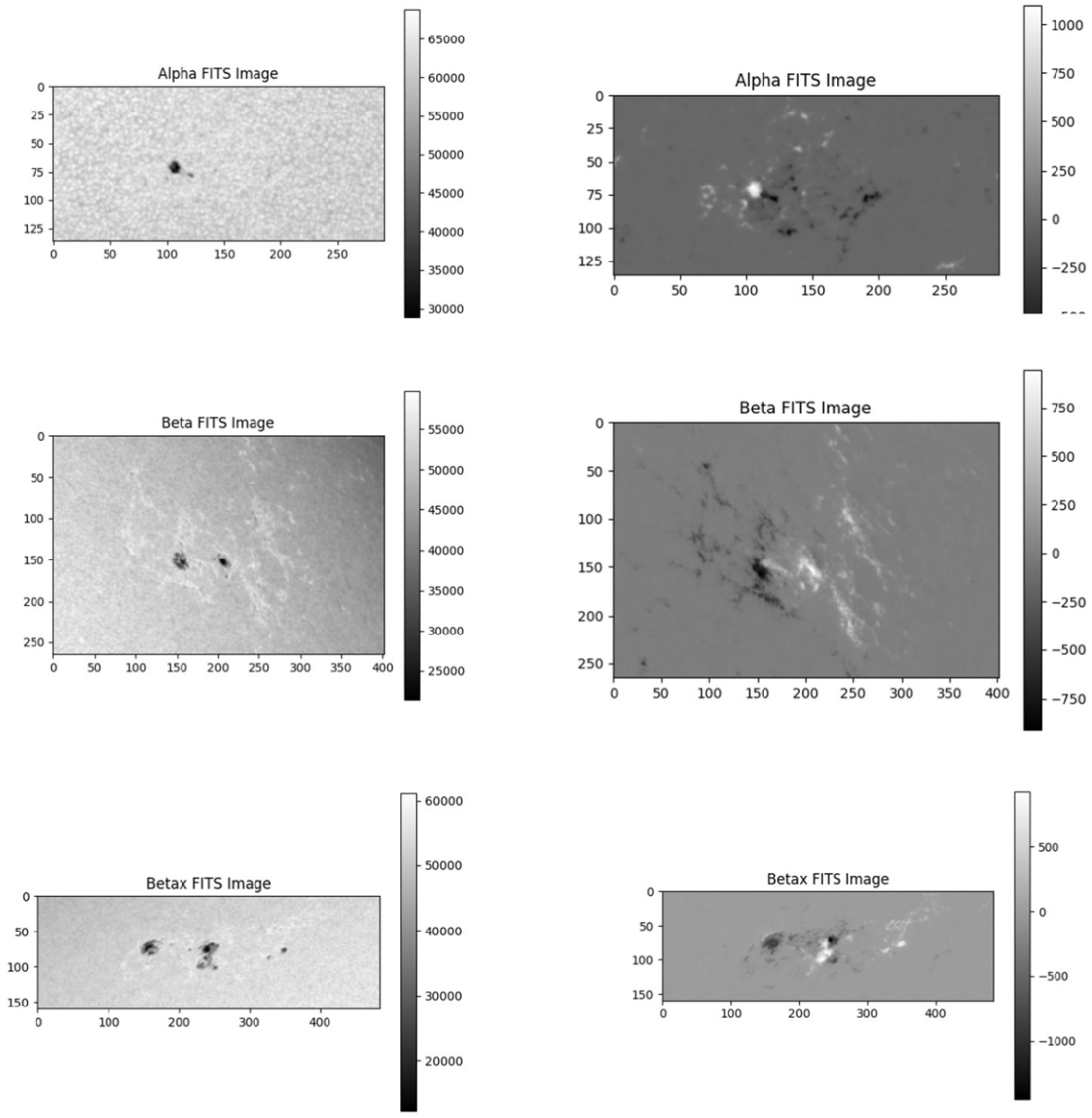

Figure 1. Sample data set, to the left are continuum images and to the right are magnetogram images.

4.2.2. ResNet Unit Combined with Convolutional Block Attention Module (CBAM)

CBAM was first introduced by Woo et al. (2018). CBAM is a lightweight module that combines both spatial and channel-wise attention mechanisms to refine feature maps. In the same process as the residual module combined with SE-Net, the CBAM module is integrated into each residual module. The structure of the residual module combined with CBAM is depicted in Figure 5.

It can be seen from the figure that when the feature map enters the module, it will first pass through channel attention and then pass through spatial attention. The process can be summarized as

$$U = M_C(F) \otimes F, \tag{1}$$

$$X = M_S(U) \otimes U. \tag{2}$$

Among them, X is the feature map after convolution, M_c is the channel attention, while assuming U is the feature map after channel attention processing, and $\otimes$ is the multiplication of corresponding elements. M_s is spatial attention, and we also assume F is the feature map after spatial attention processing. The main changes are in the feature extraction section of the residual module and the skip connection remains unchanged.

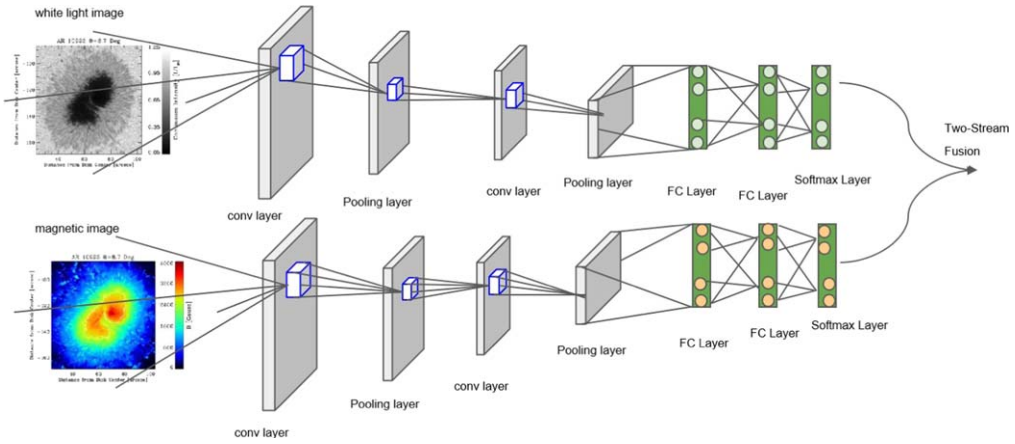

Figure 2. Structure diagram of dual-stream CNN adopted.

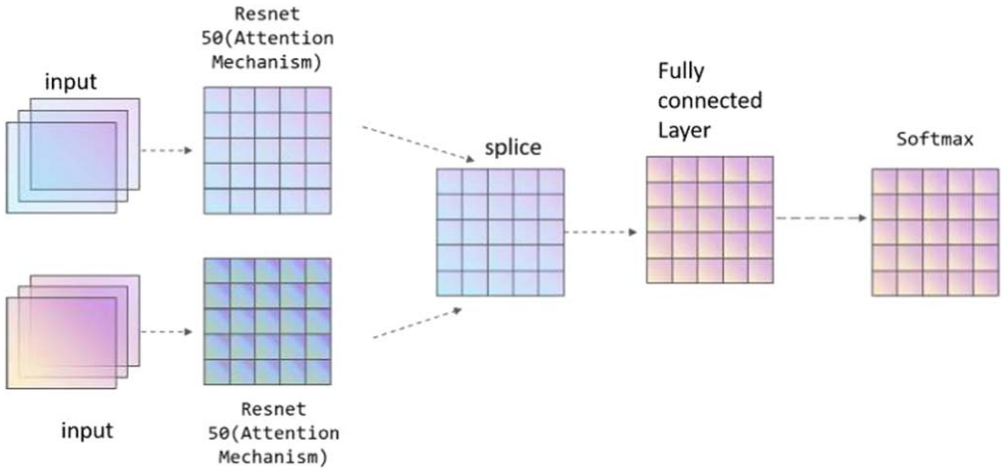

Figure 3. Structure diagram of DSCNN-AM.

4.2.3. Model Construction

During the model construction, attention mechanisms are integrated into the residual units of the ResNet50. The specific construction process involves first building separate branches: one incorporating SE-Net for channel-wise attention and another with CBAM for combined channel and spatial attention. Next, ResNet50 branches (SE-Net or CBAM) are created for extracting features from white light and magnetic images, named branch 1 and branch 2 respectively. The outputs, out1 and out2, from these branches are then spliced and processed with Flatten. The processed features are input into the fully connected layer with L2 regularization followed by the fully connected layer with Dropout. Finally, the features are fed into Softmax for classification. This construction is followed by training with ten-fold cross-validation to ensure robust evaluation and performance.

4.2.4. Model Evaluation and Fusion

Model evaluation and fusion employ a ten-fold cross-validation to ensure objective evaluation of model performance by mitigating the risk of improper data slicing. This technique divides the data set into ten parts using nine parts for training and one part for testing in each iteration, ultimately providing a robust assessment of the model's accuracy.

After training, predictions from three dual stream models, ResNet50, ResNet50 with SE-Net and ResNet50 with CBAM, are evaluated. This process provides the classification performance and corresponding results for the fused models, demonstrating superior performance compared to non-fused models.

5. Experiment and Discussion

In this section we discuss the experimental setup and results. The first group of results is of three main models: dual-stream

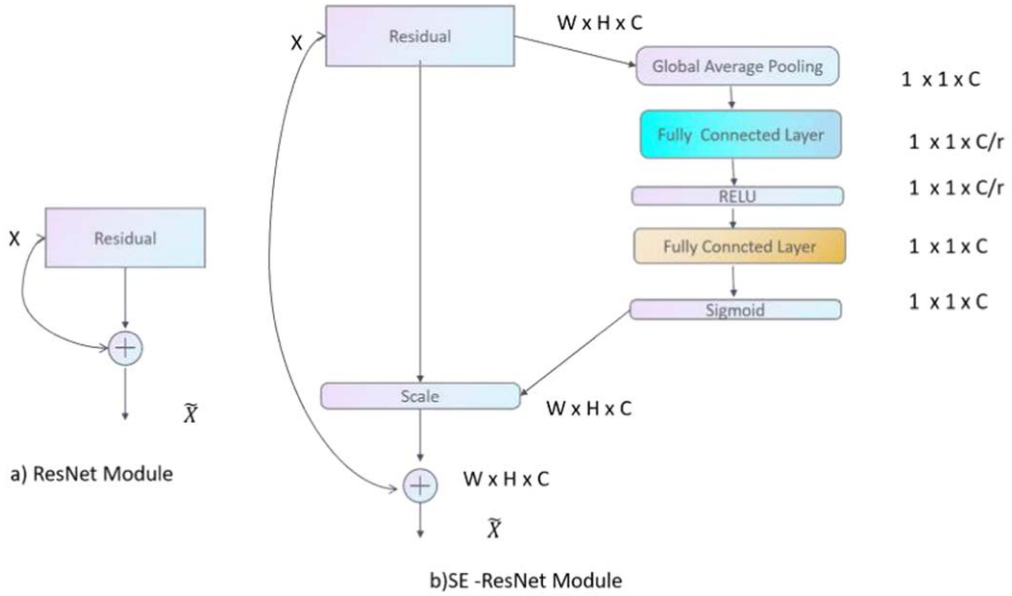

Figure 4. Residual module combined with SE-Net.

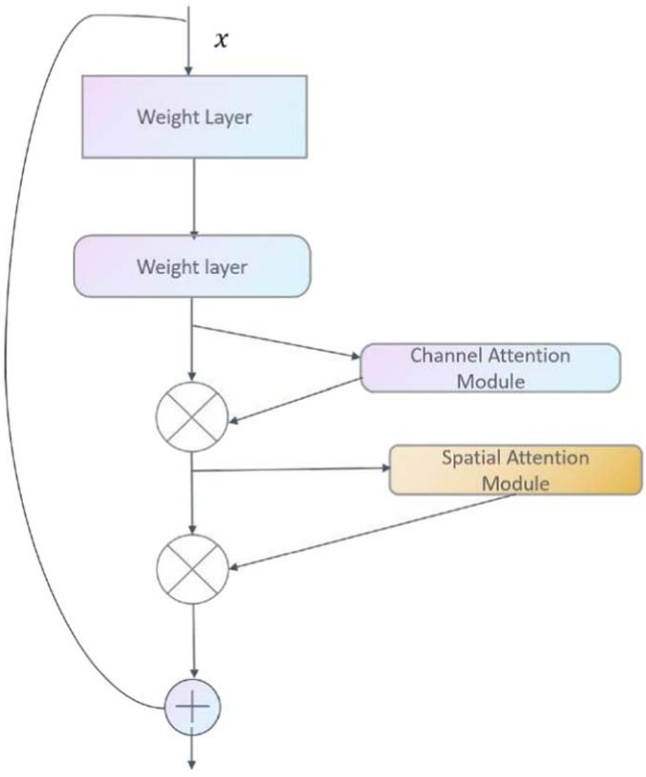

Figure 5. Residual module combined with CBAM.

ResNet50, dual-stream ResNet50 combined with SE-Net and dual-stream ResNet50 combined with CBAM. The models were trained and evaluated using both white light and magnetic images separately and in combination.

5.1. Before Model Fusion

Here we evaluate the performance of different dual-stream ResNet50 models before applying model fusion techniques. The aim is to establish a baseline for comparison and understand the impact of integrating the attention mechanism on the models' performance. Baseline Dual-stream ResNet50 uses the standard ResNet50 architecture with dual input streams for white light and magnetic maps. It provides a reference point for evaluating the effectiveness of adding the attention mechanism. The Dual-stream ResNet50 with SE-Net integrates SE-Net to improve feature recalibration by weighting the importance of different features. We investigate whether this addition brings any improvements to the performance metrics. The Dual-stream ResNet50 with CBAM introduces both channel and spatial attention mechanisms to refine feature extraction. This variant aims to enhance the model's ability to focus on relevant features in the input data. Table 1 summarizes the experimental results for each of these models providing accuracy, recall and F1-score. The goal is to analyze how the integration of SE-Net and CBAM affects the model's performance in comparison to the baseline ResNet50 model.

The inputs for the ResNet50 model are white light and magnetic images. It showed accuracy of 84.93%, recall of 84.93% and an F1-score of 84.87%. This model serves as a reference point to evaluate the performance improvements introduced by integrating SE-Net and CBAM. The SE-Net model achieved an accuracy of 84.87%, recall of 84.87%, and an F1-score of 84.41%. Compared to the baseline ResNet50 model, the SE-Net integrated model showed no significant improvement. This could be due to the equal contribution of

Table 1
Experimental Results of Each Dual-stream Model

Model	Data	Accuracy	Recall	F1-Score
Dual-stream ResNet50	White light map and magnetic map	84.93%	84.93%	84.87%
Dual-stream ResNet50 (SE-Net)	White light map and magnetic map	84.87%	84.87%	84.41%
Dual-stream ResNet50 (CBAM)	White light map and magnetic map	88.53%	88.53%	88.22%

Table 2
Fusion Experiment Results of Each Dual-stream Model

Model	Data	Accuracy	Recall	F1-Score
Dual-stream ResNet50 Fusion	White light map and magnetic map	90.61%	90.61%	90.57%
Dual-stream ResNet50 (SE-Net) Fusion	White light map and magnetic map	88.23%	88.23%	87.95%
Dual-stream ResNet50 (CBAM) Fusion	White light map and magnetic map	95.8%	96%	98%

feature maps in the classifier's view, indicating that SE-Net may not effectively enhance the classification performance for this specific task. The CBAM model achieved an accuracy of 88.53%, recall of 88.53% and an F1-score of 88.22%. This represents a significant improvement over the baseline model, with an accuracy increase of 3.6% and an F1-score increase of 3.35%. The spatial attention mechanism in CBAM likely contributed to these improvements by allowing the model to better focus on the relevant features in the images.

5.2. Model Fusion

For model fusion we used outputs from the dual-stream ResNet50, dual-stream ResNet50 (SE-Net) and dual-stream ResNet50 (CBAM) models. We performed 10-fold cross-validation and fused the results from ten small models. The results are shown in Table 2.

Comparing Tables 2 and 1, we see improvement in all indicators post-fusion. The accuracy and weighted F1-scores for the dual-stream ResNet50 improved by 5.68% and 5.7%, respectively. The dual-stream ResNet50 (SE-Net) displayed a 3.39% increase in accuracy and a 3.54% increase in weighted F1-scores. The dual-stream ResNet50 (CBAM) exhibited a 4.22% increase in accuracy and a 4.35% increase in weighted F1-scores. This indicates that model fusion enhances classification ability likely due to better utilization of the data set and the integration of various sub-model classification capabilities.

The improvements observed in the CBAM-integrated model and the fusion results highlight the importance of attention mechanisms and model fusion in enhancing classification performance of the proposed model. The spatial attention provided by CBAM allows the model to focus on the most relevant features in the sunspot images leading to better classification accuracy. Additionally, model fusion leverages the strengths of different sub-models, providing a more robust and comprehensive classification capability.

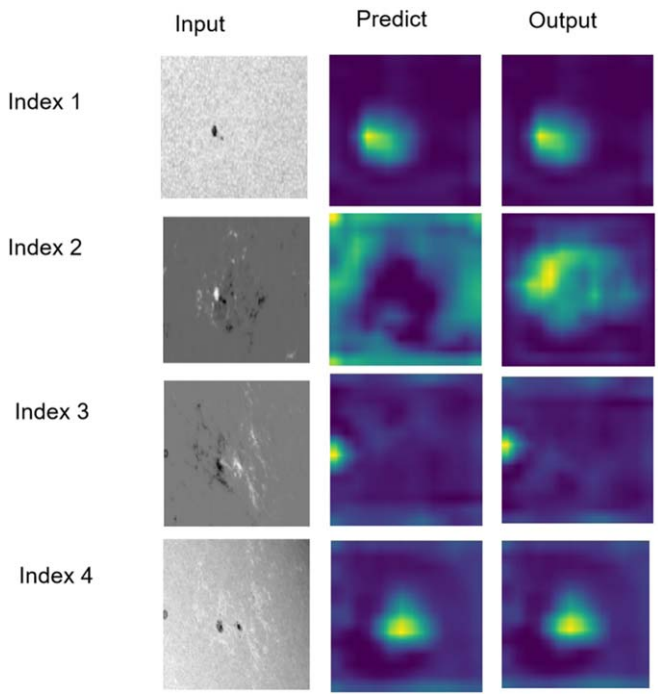

Figure 6. Heatmap of the attention mechanism output. The heatmap highlights the areas of the image that the attention mechanism focuses on, illustrating its contribution to the model's improved classification performance.

5.3. Attention Mechanism Visualization

To provide an intuitive understanding of the role of the attention mechanism in the model, we include a heatmap

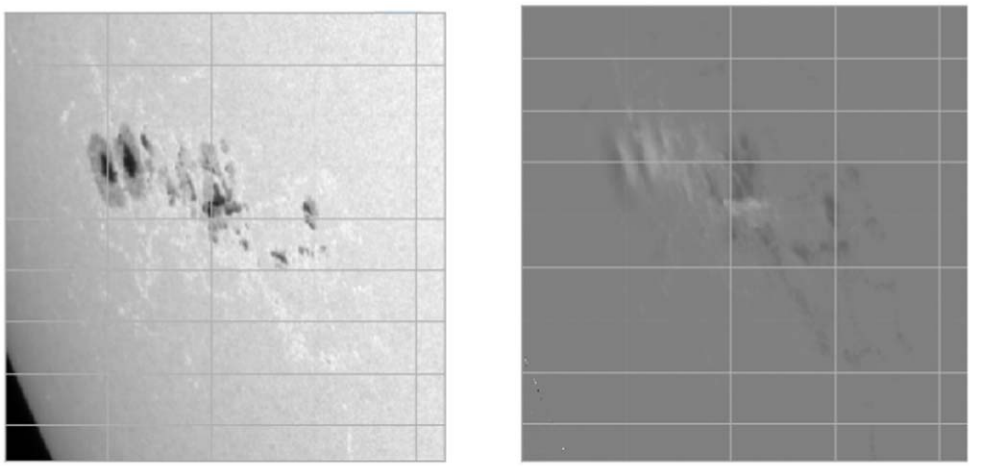

Figure 7. White light and magnetic map at the end of object No. 2048.

visualization of the attention mechanism's output. This heatmap helps illustrate how the attention mechanism focuses on different regions of the input images, thereby improving the model's classification performance. Figure 6 shows the results of the heatmap.

In this figure, four different indices of input images are displayed. For each input image, the corresponding heatmap visualizations of the attention mechanism's "Predict" and "Output" stages are shown. These visualizations demonstrate how the attention mechanism emphasizes different areas within the input image, helping to enhance the model's ability to accurately classify the images.

We take Betax class object 2048 as an example, as featured in Figure 7. The left image is a white light map of the sunspot group where features are blurred due to dimming effects and a black background. The right image is a magnetic field map (magnetogram) which also shows decreased accuracy in magnetic field strength measurement because of these effects. As sunspots progress toward the edge of the solar surface projection, edge dimming effects further blur the white light map features and reduce magnetic field measurement accuracy. When the sunspot group approaches the edge of the solar disk, image quality degradation can cause poor model classification accuracy. In cases of misclassification, the transient appearance and evolution-related disappearance of sunspots are challenging to handle manually. However, the attention mechanism in our model can mitigate the impact of these effects, including edge dimming and black background interference, thus improving classification accuracy.

We also take Alpha class object 1360 as an example, as depicted in Figure 8. The object was consistently displayed as a unipolar sunspot group over three days (a–f) and the model classification was correct. However, if on any other day another sunspot had appeared near one of the sunspots in the group, the features of the sunspot group might have been classified differently, potentially as Beta or Betax. This demonstrates that brief appearances of additional sunspots during the modeling process can lead to misclassification. The dual-stream CNN with attention mechanisms (SE-Net and CBAM) incorporated in our method helps to mitigate this issue. The attention mechanisms allow the model to focus on the most relevant features and spatial regions, reducing the impact of edge dimming effects and background interference. As a result, the model achieves more accurate classifications even when the sunspot features are blurred or evolve over time.

Additionally, we can take the Beta class object 3120 as an example, as shown in Figure 9. The initial sunspot group is clearly bipolar but during the evolution process the right sunspot gradually dissipates while the left sunspot remains. Consequently, when the image of the sunspot group at this later stage is input into the model, it is likely to be incorrectly identified as Alpha. This blurred type feature formed due to the evolution of the sunspot group may be a significant reason for the model's poor classification accuracy. In summary, the image demonstrates the challenge of classifying evolving sunspot groups. The clear initial bipolar structure evolves into a less distinct single sunspot, leading to potential misclassification. Attention mechanisms can help by focusing on the most relevant features at different stages and incorporating temporal information can further enhance the model's ability to correctly classify evolving sunspot groups.

Using the false positive rate as the horizontal axis and the true positive rate as the vertical axis, we can draw the Receiver Operating Characteristic (ROC) Curve as shown in Figure 10. Blue lines represent the ROC curves for the dual flow ResNet50, red lines represent the ROC curves for the dual

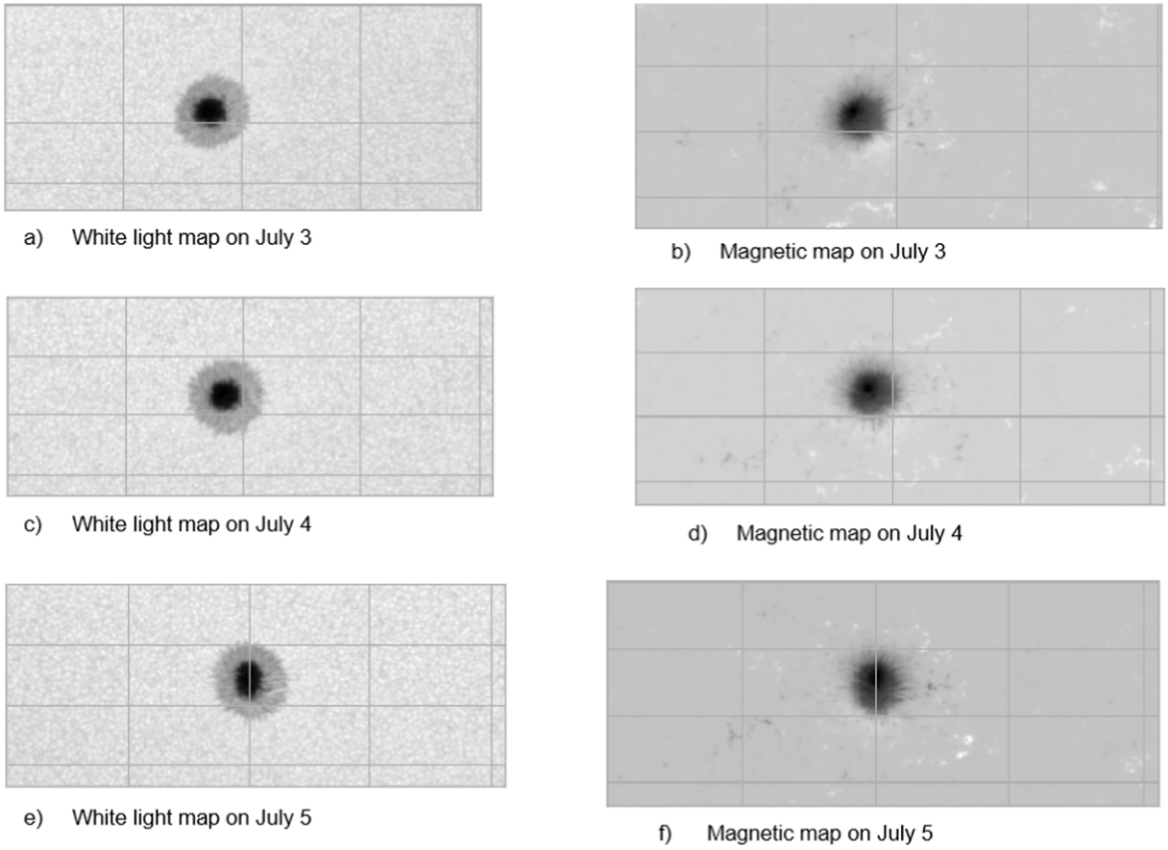

Figure 8. White light and magnetic maps of object No. 1360 in 2010 July.

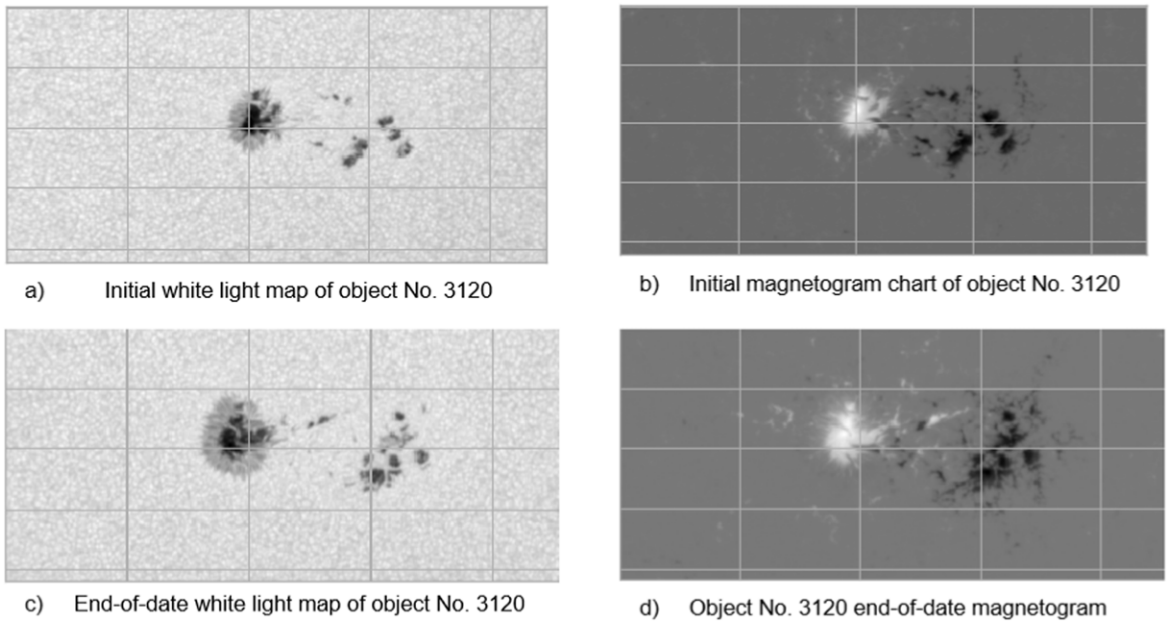

Figure 9. White light and magnetic maps of the early and late stages of object No. 3120.

Table 3
Experimental Results of Each Dual-stream Model

Model	Data	Accuracy	Recall	F1-Score
Dual-stream ResNet50	White light map and magnetic map	84.93%	84.93%	84.87%
Dual-stream ResNet50 (SE-Net)	White light map and magnetic map	84.87%	84.87%	84.41%
Dual-stream ResNet50 (CBAM)	White light map and magnetic map	88.53%	88.53%	88.22%

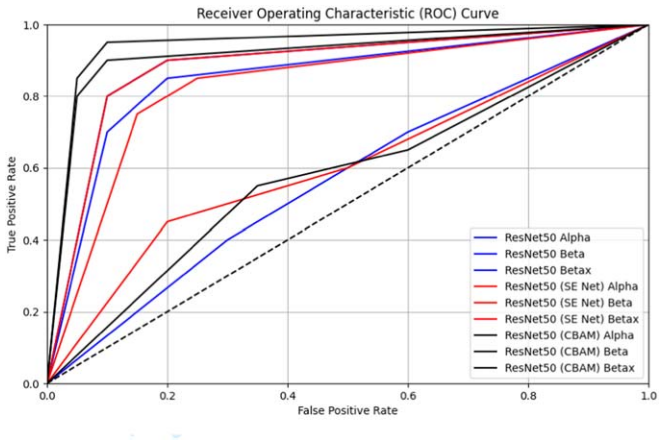

Figure 10. ROC images of the three models.

flow ResNet50 (SE-Net) and black lines represent the ROC curves for the dual flow ResNet50 (CBAM). Ideally, all categories are correctly classified as (0, 1) points so the classification results of each category in each model should be as close as possible to (0, 1). The ROC curves plot the true positive rate (vertical axis) against the false positive rate (horizontal axis) at various threshold settings. A larger Area Under Curve (AUC) indicates stronger classification performance. The dual flow ResNet50 (CBAM) shows significant improvement in AUC values for the Alpha and Betax classes compared to the other models, although the Beta class performance decreases, likely due to complex magnetic pole distributions in some Beta images. This suggests that the attention mechanism might not fully cover the magnetic pole areas, leading to biased feature extraction.

Taking the image of Betax class 6975 from the data set as an example, this image is input into the models of dual flow ResNet50, dual flow ResNet50 (SE-Net) and dual flow ResNet50 (CBAM) fusion, and the probability distribution of Softmax is directly output. The results are shown in Table 3.

From Table 3, it can be seen that the object 6975 with edge dimming is determined as Beta by both dual flow ResNet50 and dual flow ResNet50 (SE-Net) with decision probabilities above 90%. This indicates that the network with SE-Net added only gives channel weights to the feature map which is not sufficient to extract effective classification features. On the other hand, the dual-stream ResNet50 (CBAM) correctly classifies the image as Betax with a probability of 75.43%, which is significantly higher than the probabilities for Alpha and Beta. This suggests that when dealing with images featuring edge dimming, spatial attention can better capture features conducive to accurate classification.

5.4. Comparative Analysis of Sunspot Detection and Classification Methods

The methods by Chola & Benifa (2022), Veeramani & Sudhakar (2024) and the proposed approach all aim to improve the accuracy and reliability of sunspot detection and classification.

This study aims to compare these methods based on their classification accuracy, precision, recall, F1-score and other relevant metrics. By evaluating these approaches, we were able to identify the strengths and limitations of each method, thus providing valuable insights into the effectiveness of different techniques in the field of sunspot detection and classification. This comparative analysis will contribute to ongoing efforts to develop robust and reliable systems for solar activity monitoring and research.

Table 4 highlights the strengths and weaknesses of each method. Chola et al.'s approach using AlexNet-based deep convolutional networks achieves outstanding classification performance with near-perfect accuracy, precision, recall and F1-score values. Veeramani et al.'s method which relies on a pre-processing and differencing approach also demonstrates excellent performance with high accuracy, specificity, sensitivity, precision and F1-score as well as a low Dice loss. The proposed method, using dual stream ResNet50 with SE-Net and CBAM attention mechanisms shows robust performance in solving the edge dimming cases with the CBAM variant providing the best results in terms of accuracy and F1-score.

The Recall and F1-score Curve as shown in Figure 11 highlights the trade-offs between recall and F1-score for each method.

The bar chart in Figure 12 shows the accuracy comparison for each method.

By integrating these results into a comprehensive evaluation, we better understand the capabilities and limitations of each

Table 4
Comparison of Sunspot Detection and Classification Methods

Method	Dataset	Model	Accuracy	Recall	F1-Score
AlexNet (Chola et al. 2022)	HMI, MDI	AlexNet-based CNN	99.71%	100%	100%
Veeramani et al. (2024)	FITS (HMI Images)	Preprocessing-based method	99.62%	99.86%	99.41%
Dual-stream ResNet50 Fusion	HMI	ResNet50-based dual stream CNN	90.61%	90.61%	90.57%
Dual-stream ResNet50 (SE-Net) Fusion	HMI	ResNet50 with SE-Net	88.23%	88.23%	87.95%
Dual-stream ResNet50 (CBAM) Fusion	HMI	ResNet50 with CBAM	95.8%	96%	98%

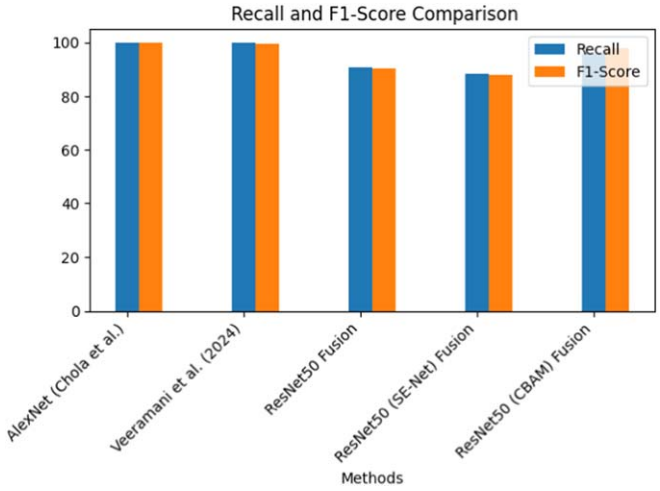

Figure 11. The Precision-Recall Curve.

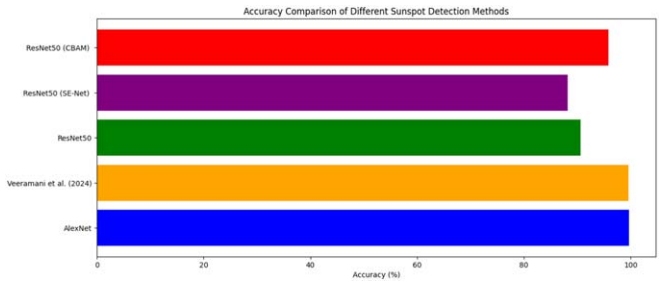

Figure 12. A bar chart comparing root mean square error (RMSE) and mean absolute error (MAE) values.

method, facilitating the development of more effective and accurate models for solar activity monitoring.

6. Conclusion

We improve on the dual flow ResNet50 by adding SE-Net and CBAM respectively to the residual network, thus forming two new models and comparing them with the dual stream ResNet50. The accuracy, F1-score, recall and ROC curve are used to evaluate the advantages and disadvantages of the model. As noted, the added CBAM has better classification performance because it contains spatial attention. The experimental results also show that model fusion helps improve the performance of the model.

7. Future Work

In this paper, deep learning is applied for classifying the magnetic types of sunspot groups. Despite progress, training time remains long with each epoch training taking 4 hr due to network complexity. Future work should focus on reducing network complexity without compromising accuracy. Additionally, since only the circular area of the Sun image is relevant and the rest is black, solutions to mitigate the impact of this black background are needed.

For more accurate predictions, high-quality data are crucial as magnetic type classification impacts solar storm prediction. Future research should involve creating a large high-quality data set of sunspot magnetic types.

Acknowledgments

I would like to express my sincere gratitude to my Supervisor Prof. Tian Wei Xin for his invaluable guidance, continuous support and encouragement throughout the course of my research. His insightful feedback and expertise were instrumental in shaping this work. I would also like to thank Li Junlin, for his assistance in various aspects of the research. His willingness to answer my questions and provide advice whenever needed has been greatly appreciated.

References

Abed, A. K., Qahwaji, R., & Abed, A. 2021, AdSpR, 67, 2544
Anderson, P., He, X., Buehler, C., et al. 2018, in Proc. of the IEEE Conf. on Computer Vision and Pattern Recognition (New York: IEEE), 6077
Chola, C., & Benifa, J. B. 2022, GloTP, 3, 177
Colak, T., & Qahwaji, R. 2008, SoPh, 248, 277
Fang, Y., Cui, Y., & Ao, X. 2019, AdAst, 2019, 9196234
Goodfellow, I., Bengio, Y., & Courville, A. 2016, Deep Learning (Cambridge, MA: MIT Press)

Guo, J., Lin, J., & Deng, Y. 2014, MNRAS, 441, 2208
Herrera, V. V., Soon, W., & Legates, D. 2021, AdSpR, 68, 1485
Hu, J., Shen, L., & Sun, G. 2018, Proc. of the IEEE Conf. on Computer Vision and Pattern Recognition (New York: IEEE), 7132
Jaeggli, S. A., & Norton, A. A. 2016, ApJL, 820, L11
Junior, D., & Luisir, S. 2019, Enhancing solar flare forecasting: A multi-class and multi-label classification approach to handle imbalanced time series in Proc. Conf. Solar Physics Mach. Lear. (São Carlos, Brazil: UFSCar)
Kucuk, A., Banda, J. M., & Angryk, R. A. 2017, Artificial Intelligence and Soft Computing: 16th Int. Conf., ICAISC (Berlin: Springer), 118
Lee, K., Moon, Y.-J., Lee, J.-Y., Lee, K.-S., & Na, H. 2012, SoPh, 281, 639
Ling, L., Yan-mei, C., Si-qing, L., & Lei, L. 2020, ChJAA, 44, 462
Majed, S. F., Abd, M. A., & Zharkova, V. 2010, Technological Developments in Networking, Education and Automation (Berlin: Springer), 297
Mourato, A., Faria, J., & Ventura, R. 2024, Eng. Appl. Artif. Intell., 129, 107636
Ndacyayisenga, T., Umuhire, A. C., Uwamahoro, J., & Monstein, C. 2021, Annales Geophysicae, 39, 945, Copernicus GmbH
Nguyen, S. H., Nguyen, T. T., & Nguyen, H. S. 2005, Rough Sets, Fuzzy Sets, Data Mining, and Granular Computing: 10th Int. Conf., RSFDGrC (Berlin: Springer), 263
Nguyen, T. T., Willis, C. P., Paddon, D. J., & Nguyen, H. S. 2006, 2006 Int. Conf. on Hybrid Information Technology, Vol. 2 (Piscataway, NJ: IEEE), 257
Prasad, S. S., Deo, R. C., Downs, N., et al. 2022, IEEEA, 10, 24704
Schuh, M. A., & Angryk, R. A. 2014, Massive Labeled Solar Image Data Benchmarks for Automated Feature Recognition in 2014 IEEE Int. Conf. Big Data (Big Data) (Washington, DC: IEEE)
Stenning, D., Kashyap, V., Lee, T. C., van Dyk, D. A., & Young, C. A. 2012, in Statistical Challenges in Modern Astronomy V (Berlin: Springer), 329
Tang, R., Zeng, X., Chen, Z., et al. 2021, ApJS, 257, 38
Veeramani, M., & Sudhakar, M. 2024, NewA, 105, 102089
Woo, S., Park, J., Lee, J.-Y., & Kweon, I. S. 2018, Proc. of the European Conf. on Computer Vision (ECCV) (Berlin: Springer), 3
Xu, Y., Jia, R., Mou, L., et al. 2016, arXiv:1601.03651
Yi, K., Moon, Y.-J., Lim, D., Park, E., & Lee, H. 2021, ApJ, 910, 8